EEG-based Transceiver Design with Data Decomposition for Healthcare IoT Applications

EEG-based Transceiver Design with Data Decomposition for Healthcare IoT Applications

Alaa Awad Abdellatif*†, Mohammad Galal Khafagy*, Amr Mohamed*, and Carla-Fabiana Chiasserini†
*Department of Computer Science and Engineering, Qatar University, Doha, Qatar
†Department of Electronics and Telecommunications, Politecnico di Torino, Torino, Italy
E-mail: aawad, mkhafagy, amrm@qu.edu.qa and chiasserini@polito.it

***Abstract*—The emergence of Internet of Things (IoT) applications and rapid advances in wireless communication technologies have motivated a paradigm shift in the development of viable applications such as mobile-Health. These applications boost the opportunity for ubiquitous real-time monitoring using different data types such as Electroencephalography (EEG), Electrocardiography (ECG), etc. However, many remote monitoring applications require continuous sensing for different signals and vital signs, which result in generating large volumes of real time data that requires to be processed, recorded, and transmitted. Thus, designing efficient transceivers is crucial to reduce transmission delay and energy through leveraging data reduction techniques. In this context, we propose an efficient data-specific transceiver design that leverages the inherent characteristics of the generated data at the physical layer to reduce transmitted data size without significant overheads. The goal is to adaptively reduce the amount of data that needs to be transmitted in order to efficiently communicate and possibly store information, while maintaining the required application Quality-of-Service (QoS) requirements. Our results show the excellent performance of the proposed design in terms of data reduction gain, signal distortion, low complexity, and the advantages that it exhibits with respect to state-of-the-art techniques since we could obtain about 50% compression ratio at 0% distortion and sample error rate.**

***Index Terms*—EEG signal, mobile-Health system, data compression, OFDM transceiver, signal decomposition.**

I. Introduction

The rapid advances in Edge Computing, communication technologies, Internet of Medical Things (IoMT), and Big Data have facilitated the development of Mobile-health (m-health) systems that support gathering, delivery, and retrieval of healthcare information. M-health systems leveraging the wide range of mobile technologies (e.g., smartphones, tablets, and portable health devices) enable providing efficient continuous-remote healthcare services, or known as ubiquitous healthcare [1][2]. M-Health applications are expected to inspire fundamental transformations for the healthcare industry toward Healthcare Industry 4.0 (Health 4.0) [3], especially in pre-hospital emergency care situations and for geographically remote areas. The main goal of Health 4.0 is to enable the automation and personalization of all medical processes through leveraging medical cyber-physical systems, IoMT, and Edge/Cloud computing. Health 4.0 allows, on one hand, patients to monitor their health without the necessity of visiting the hospital or clinic. On the other hand, the hospitals/caregivers can provide patients with medical services through computerized medical information systems.

Despite these major trends, new challenges have emerged due to the massive real-time data collected as part of health monitoring systems. Healthcare applications require processing and wireless delivery of intensive data to ensure the quality of healthcare services. This obviously sets a significant load on the system design in terms of processing capabilities, storage space, and power consumption. In addition to that, m-health systems typically consist of several battery-operated devices that should run for a long time without replacement, hence enabling transmission of large volumes of data in such systems continuously increases the energy consumption and complexity of radio frequency (RF) transceivers.

To address this shortcoming and meet diverse requirements of next-generation wireless networks, and IoMT applications, different modules of physical layer need to be optimized so that they can be flexibly configured based on the technical requirements of each application. In this context, this paper proposes an efficient EEG-based transceiver design that maintains application Quality-of-Service (QoS) requirements (i.e., signal distortion) taking into consideration the characteristics of the acquired data, while saving a significant amount of transmitted data. We argue here that devoting transceiver design to be specific for a certain type of data (e.g., EEG) is perfectly in consistence with IoMT devices that mostly acquire one type of data efficiently (e.g., using Emotiv headset, or QardioCore wireless Electrocardiography (ECG) monitor). Hence, leveraging the characteristics of such data at the physical layer will have positive effects on the costs as well as on the energy consumption of the RF transceiver. Herein, we focus on EEG signal, which is the main source of information on brain electrical activities that play an important role in the diagnosis of several brain disorders [4], and have a primary role in Brain Computer Interface (BCI) applications [5][6]. Thus, our main contributions can be summarized as follows:

1) Design an efficient EEG-based transceiver that leverages the characteristics of the EEG signals at the physical layer in order to provide an efficient transmission, while maintaining application level QoS. Leveraging the exiting orthogonal frequency division multiplexing (OFDM) transceiver's components, the

proposed method performs the data compression task as part of the physical layer, hence leading to an efficient compression scheme with no significant overhead.
2) Decompose generated data into multiple streams to further increase compression ratio through applying different compression thresholds for each stream, and discovering the dependency between different streams.
3) Analytical proof that the applied signal decomposition scheme results in increased optimal lossless compression ratio.
4) The proposed design is evaluated through simulations discussing the tradeoff between transmitted data length and signal distortion. Our results show the gain provided by our solution, and its ability to obtain high lossless and lossy compression ratios.

The rest of the paper is organized as follows. Section II discusses the related work while highlighting the novelty of our work. Section III describes system model. Section IV illustrates proposed data decomposition and knowledge discovery scheme. Section V presents EEG signal characteristics and proposed EEG transceiver design with threshold-based compression, as well as stream-based compression schemes. Section VI provides our simulation results and discussion, while Section VII concludes the paper.

II. Related Work

In the era of IoMT and Industry 4.0, the rapid advances in data volumes, cloud storage, edge computing, and ubiquitous network connectivity have enabled gathering, storing, and analysis of large volumes of operational data that was previously impossible. A key aspect in achieving the anticipated goals of Industry 4.0 is data processing. Given the expected volumes of gathered data, the provision of valuable services is challenging without adequate information processing and management. This is also manifested through the leading International Patent Classification (IPC) analysis, where G06F19/00 category (i.e., digital computing or data processing equipment or methods, specially adapted for specific applications) is ranked fifth in the top 20 technical IPC categories, with 130 patents between January 2006 and December 2015 [7]. Furthermore, reducing the amount of transmitted data is essential for battery-operated IoMT devices in order to save transmission energy. Some promising approaches in this context are: (i) performing local in-network processing and compression on the gathered data before transmission, including compressive sensing (CS) [8][9][10], (ii) leveraging deep learning as a powerful tool for machine learning and health informatics to generate optimized high-level features and semantic interpretation from the gathered data [11].

In CS, sampling is performed by multiplying the original signal with a linear embedding matrix, hence, the high-dimensional data vector is projected into a low-dimensional subspace. Although, CS has shown great promise for providing high compression ratio, the construction of CS-based hardware is challenging [12]. In particular, the signal reconstruction requires in general high computational cost, which limits the use of CS in strictly real-time applications [13]. As an example, the Orthogonal Matching Pursuit (OMP) technique for signal reconstruction involves heavy matrix computation (see, e.g., [14] for details). Furthermore, there is a tradeoff between hardware energy-efficiency and signal recovery accuracy. For instance, if a data-driven optimization method (e.g., NuMax [15]) is used for improving signal recovery accuracy, more hardware power consumption is expected. On the contrary, if non-data-driven random Boolean embedding is applied for enhancing hardware energy-efficiency, high recovery accuracy cannot be guaranteed [16].

Relevant to our work are also the compression techniques that have been proposed in the literature specifically for e-health applications and that are summarized in Table I. Such techniques differ in computational complexity, lossy and lossless characteristics, as well as the used waveform transformation (e.g., Fourier or wavelet transforms, vector quantization, or discrete cosine transform). In short, most of the existing work on compression is applied at the higher layers, while ignoring lower layers features (e.g., characteristics of wireless channels, signal-to-interference-plus-noise ratio (SINR), and bit/symbol error rate). Also, consequent computational complexity might turn implementing such schemes on battery-operated devices costly.

On the other hand, designing application-specific transceivers has recently gained interest. There are some efforts on enhancing future transceivers architecture to cope with long-range IoT communication and multi-standard RF transceivers, while providing high degree of scalability, flexibility, and reusability [24][25]. For instance, SRT Marine Systems granted reversible radio transceiver US patent 9473197 and European patent EP2951930 for its reversible time domain duplex (RTDD) transceiver technology. This technology enables a specific single RF architecture to be used simultaneously for both receiving and transmitting through electronic reversing of the RF chain between receive and transmit. This could be maintained through a complex combination of intelligent selection of intermediate frequencies and ultra-fast switching. Also, SRT Marine Technology Ltd of Bristol recently obtained a patent for a radio transceiver which enables multiple transceivers to share a single antenna in order to reduce costs and installation effort (GB patent no. 2460012). In the field of fiber-optic communications, [26] provides a transceiver for: (a) transmitting combined data and time code information over a fiber-optic communication means, and (b) receiving combined data and time code information from the fiber-optic communication means. In [27], the inventors present a transmitter that can receive digital audio and program information input from a plurality of sources and simultaneously broadcast a plurality of digital audio and program information signals over a limited range, hence, a user can enjoy listening to

TABLE I
SUMMARY OF COMPRESSION TECHNIQUES FOR E-HEALTH APPLICATIONS

Application	Collected Data	Description	Advantages	Limitations
Health monitoring using wearable devices [17]	Vital signals, such as respiratory rates, and ECG	Design an online signal compression algorithm using online codebook for efficient representation of data patterns	Achieve high compression ratios with little computation	Large use of memory space
Compression of biometric signals [18]	ECG	Develop lossy compression algorithm using denoising autoencoders for biometric signals compression	Computationally lightweight	Limited to signals with a certain degree of periodicity
EEG remote monitoring [19]	EEG signals	Neural network-based compression algorithms proposed for near-lossless EEG signals compression using diverse neural network and linear predictors	Reduced demand for memory space and network bandwidth	Using neural networks for prediction requires training and adding computational overhead
ECG remote monitoring [20]	ECG	DCT based compression algorithm is proposed leveraging DCT comparison between different ECG peaks	Efficient ECG compression	Processing of the DCT coefficients is energy prohibitive
EEG Compression and Seizure detection [21]	EEG	Using discrete wavelet transform (DWT) and dynamic reference lists to transmit decorrelated subband coefficients, while opting Set partitioning in hierarchical trees (SPIHT) as a source coder	Compressing EEG channels in one dimension (1-D), while also detecting seizure activities	Overhead added for decoding the data at the receivers side
Mental disorders monitoring [22]	EEG	Lightweight 1.5-D multi-channel EEG compression proposed using 1-D DWT and 2-D No List SPIHT arranging method exploiting correlations of wavelet coefficients	Enhance compression ratios with lower distortion while reducing power consumption	Limited performance compared to 2-D SPIHT algorithm in the near-lossless compression
Patient remote monitoring [23]	Electromyography (EMG) and EEG	Lossy compression scheme for multidimensional biomedical signals is proposed using codebook-excited linear prediction approach and signals modeling as filtered noise	Leveraging intra- and inter-channel redundancy in time and space	Complexity and processing delay increase linearly with number of considered channels

the digital audio, while enabling portable reception of the service within a localized setting.

In this context, one of the key components for the proposed transceiver design is reducing transmitted data size without adding additional hardware, while retaining the ability to reconstruct the original data from the received sequence. Also, equipped with accelerated Fast Fourier Transform (FFT) blocks, most of the current and future transceivers architecture [28][29] have the opportunity to leverage such a concept at the physical layer, saving significant amount of energy consumption and computational overheads. Our results can also be extended to have a significant practical impact in many big data domains, since most video, audio, and medical images are compressible or sparse in nature, hence, they can benefit from such compression scheme through leveraging the acquired data characteristics in the physical layer of the wireless transceiver. However, new challenges such as the effect of quantization and modulation have to be tackled at the physical layer to achieve such adaptive compression.

III. System Model

This paper proposes an efficient transceiver design that relies on OFDM technology while obtaining an adaptive compression method in order to control the size of the transmitted data. OFDM is a well designed technology for high-rate wireless communication. However, the performance of such systems is generally limited by the available transmission energy. Thus, we can save in energy consumption through compressing the data before transmission, while retrieving the original data at the receiver side with zero or low distortion depending on the applied compression ratio and application requirements.

The proposed system architecture, shown in Figure 1, depicts the end-to-end system from the EEG data acquisition to the M-Health Cloud (MHC). The EEG data acquisition is performed using an EEG Headset [30]; the signal is then sampled, quantized, and transmitted to the MHC through our proposed threshold-based transceiver. The main modules composing our system are described below.

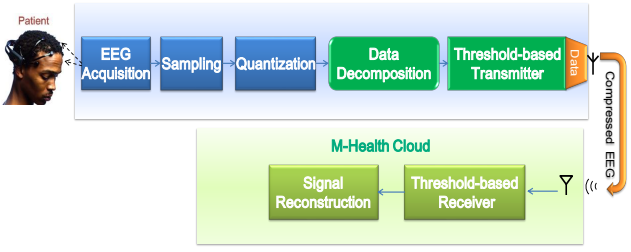

Fig. 1. System model under study.

Sampling: Let the original continuous-time electroencephalography (EEG) waveform $s(t)$ have a duration of T seconds. The waveform is sampled at a constant interval of T_s seconds to yield N_s discrete-time consecutive samples. The sampling frequency is then given as $F_s = \frac{1}{T_s}$ Hz. Hence,

$$s_n = s(t)\ \delta\left(t - nT_s\right) = s(nT_s), \tag{1}$$

TABLE II
SUMMARY OF USED NOTATIONS.

Notation	Definition
T	EEG waveform duration
N_s	Number of samples
$F_s = N_s/T$ Hz	Sampling Frequency
T_s	Inter-sample duration
L	Number of bits per sample
M	Number of symbols per sample
$K = L/M$	Number of bits per symbol

for $n \in \{0, 1, \cdots, N_s - 1\}$, where $\delta(\cdot)$ is the Dirac delta function. Our adopted notations are reported in Table II.

Quantization: The continuous amplitude of each sampled signal is quantized using an L-bit analog-to-digital converter (ADC) to one of 2^L levels, yielding the quantized signal $\tilde{x}_n$ at time index n. Each signal $\tilde{x}_n$ holds a signed integer value in the range $\{-2^{L-1}, \cdots, 2^{L-1} - 1\}$. We can express the quantized signal in vector form as

$$\underset{N_s \times 1}{\tilde{\boldsymbol{x}}} = \begin{bmatrix} x_0 & x_1 & \cdots & x_{N_s-1} \end{bmatrix}^{\mathrm{T}}. \tag{2}$$

Data decomposition: The collected EEG quantized samples are written as a sequence of symbols that depend on the adopted modulation. Such symbols are then divided into multiple streams, which are processed using Formal Concept Analysis in order to discover the correlation existing between the different streams. The streams that are found to be independent of each other, are compressed and transmitted, while others are discarded. Additionally, each stream is compressed separately, using a compression threshold that suits its characteristics, thus further increasing the compression ratio.

Threshold-based transceiver: To comply with the current and future trends, we start from the typical OFDM transceiver architecture [31] (depicted in Figure 2-(a)), and add two simple blocks: the Threshold-based Compression (TBC) and the FFT Vector Reconstruction (see Figure 2). Nevertheless, our solution can be applied to other transceiver architectures such as the one adopted by the IEEE802.11ah [24] and the IEEE802.15.4g standards [29].

In the proposed transceiver architecture, it is assumed that the available quantized samples are encoded into an unsigned binary sequence via the L-bit ADC. We first turn the generated signed-integer samples into non-negative integers by a simple shift, i.e.,

$$x_n = \tilde{x}_n + 2^{L-1}. \tag{3}$$

Then the symbols are forwarded to the modulation and IFFT modules. Details on the TBC and FFT vector reconstruction blocks are discussed in the following section.

IV. Data Decomposition and Knowledge Discovery

In this section, we leverage the physical layer's characteristics to decompose quantized EEG samples into multiple streams of symbols, such that the dependency between different streams can be reduced, hence, increase compressibility.

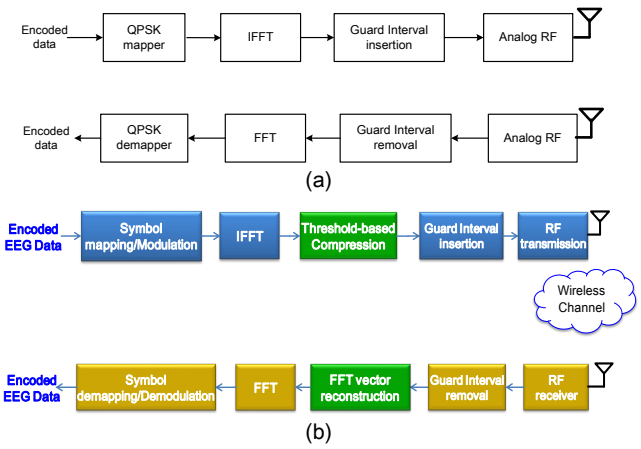

Fig. 2. Block diagram of (a) the transceiver architecture for IEEE802.11ah systems [24], (b) the adopted EEG transceiver.

A. Data Decomposition

We first decompose the EEG signal x_n into multiple streams of symbols x^m, for $m \in \{1, 2, \cdots, M\}$. Let the binary encoded sequence of x_n be denoted as $\boldsymbol{b} \in \mathbb{F}_{2^L}$, with $\mathbb{F}_p$ being the Galois Field of order p. Hence, $\boldsymbol{b}$ is a sequence of L bits on the form

$$\boldsymbol{b} = \overbrace{\Big[\underbrace{\mathrm{b}_{\mathrm{K}-1}^{(\mathrm{M}-1)} \cdots \mathrm{b}_0^{(\mathrm{M}-1)}}_{\boldsymbol{b}^{(M-1)}} \quad \cdots \quad \underbrace{\mathrm{b}_{\mathrm{K}-1}^{(0)} \cdots \mathrm{b}_0^{(0)}}_{\boldsymbol{b}^{(0)}}\Big]}^{L \text{ bits}} \tag{4}$$

where $\boldsymbol{b}^{(m)}$ is the group of K bits composing the m-th symbol, with $m \in \{1, \cdots, M\}$, where K and M depend on the modulation type. More specifically, M is the number of symbols per sample, which depends, not only on the modulation order O, but also on the number of bits per sample L, as follows:

$$M = \frac{L}{\log_2(O)} = \frac{L}{K}. \tag{5}$$

Then, x_n can be rewritten as:

$$x_n = \sum_{m=0}^{M-1} \sum_{k=0}^{K-1} 2^{mK+k} b_k^{(m)} = \sum_{m=0}^{M-1} 2^{mK} x^m, \tag{6}$$

with

$$x^m = \sum_{k=0}^{K-1} 2^k b_k^{(m)}. \tag{7}$$

In conclusion, the bit stream block $\boldsymbol{b}^{(m)}$ is simply the binary representation of x^m, which implies $x^m \in \{0, 1, \cdots, 2^K - 1\}$.

B. Knowledge Discovery

Leveraging the symbol streams that we have created, the compression ratio can be further increased by discovering the correlation between different streams. In a nutshell, using Formal Concept Analysis (FCA) for knowledge discovery [32], we select the minimal-representative streams

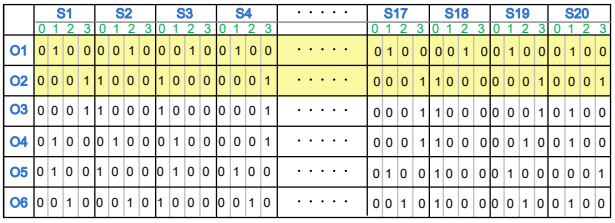

Fig. 3. Steps 1 and 2: Transformation of generated streams into a binary relation, and identification of identified formal concepts (highlighted in colors).

so as to the number of transmitted data streams without losing knowledge.

We start by introducing the basic notions used to induce a binary relation between the generated streams. Let $\mathcal{O}$ be the set of streams (i.e., objects), $\mathcal{A}$ the set of symbols' values (i.e., attributes), and I the binary relation on the universe $\mathcal{U} = \mathcal{O} \times \mathcal{A}$ that defines which objects have which attributes. In order to transform our streams into formal context of $(\mathcal{O}, \mathcal{A}, I)$, we consider the attributes a_v of each symbol s to be all the possible values it may take, depending on the employed modulation, for $v \in \{0, 1, \cdots, 2^K - 1\}$, and $a_v \in \{0, 1\}$. Thus, the vector of attributes $\mathcal{A}$ for each stream x^m is defined as

$$\mathcal{A}(\tilde{x}^m) = \left[\underbrace{a_0 \cdots a_{2^K-1}}_{s_1} \quad \cdots \quad \underbrace{a_0 \cdots a_{2^K-1}}_{s_{N_s}} \right], \quad (8)$$

where $\mathcal{A}$ represents the possible values of each symbol.

Our aim is to obtain the dependency between different streams through finding the minimal set of formal concepts[1] covering our relation. Herein, we refer to the implications as the minimal set of rules, by which we can infer some attributes from others. We can derive formal concepts from our formal context using the derivation operators or difunctional decomposition[2] [33][34]. Once the formal concepts are derived, implications can be identified, hence transmitting only the minimal-representative number of streams. For the sake of clarity, we describe the adopted procedure by referring to a toy example where a data length of 20 samples with QPSK modulation is considered.

Step 1: Generation of formal context. Consider the generated streams of symbols. We consider each stream as an object with attributes corresponding to its symbols' values. As an example, Figure 3 illustrates the formal context of 6 streams with 20 symbols.

Step 2: Identifying formal concepts. The generated binary relation are then decomposed into a set of concepts, using the algorithm presented in [33]. However, in order to well identify the dependency between different streams, we leverage what we called *shadow concept*: we consider not only the attributes for which the relation I is equal to 1, but also the negation of the attributes, i.e., the attributes values for which the relation is equal to 0. In this case, both the attributes and the negation of the attributes form the identified concept.

Step 3: From concepts to implications. Based on the identified concepts, we derive the implications that can be used to effectively eliminate the streams that can be retrieved at the receiver using their implications with other received streams. For instance, looking at Figure 3, we can easily identify from the obtained concept that $O_2 \rightarrow O_1$, where $\rightarrow$ stands for the implications, since $O_2 = O_1 + 2$, for $O_2, O_1 \in [0, \cdots, 3]$.

Step 4: Elimination. For each obtained concept, we transmit only one stream and eliminate other streams that belong to the same concept. Then, the retrieval process is done at the receiver using identified implications.

Proposition 1: *Decomposing EEG signal $\boldsymbol{x}$ into multiple streams of symbols $\boldsymbol{x}^m$ results in increasing compressibility of the signal.*

Proof: See Appendix A. ∎

This proposition proves that leveraging the decomposition of original data $\boldsymbol{x}$ into multiple streams $\boldsymbol{x}^m$ with identifying the dependency between different streams results always in lower entropy in each stream than the entropy of original data, hence, increasing compression ratio. This corresponds to the reduction in uncertainty of each stream arising from the decomposition with knowledge discovery process. This reduced uncertainty is quantified in a lower entropy and higher compression ratio.

V. Threshold-based EEG Transceiver Design

In what follows, we propose an efficient, low-complexity and reconfigurable EEG transceiver design. The proposed transceiver provides an adaptive threshold-based compression taking into account the EEG sparsity feature, characteristics of the generated traffic, and physical layer components.

A. EEG Signal Characteristics

We first visualize and analyze the EEG signal in the time and frequency domains in order to understand its properties and obtain the best approach of processing and transmission. A normal continuous EEG signal in the time domain is shown in Figure 4. Using frequency domain analysis, we can significantly reduce the amount of data to be transmitted. This can be done through transforming the collected EEG data into the frequency domain using FFT [35], which is a classic frequency analysis method with complexity $O(N \log N)$.

Looking at the generated spectrum shown in Figure 5, we observe that it is to some extent sparse, or compressible[3]. Thus, we can efficiently reduce transmission energy

[1] (O,A) is a formal concept if A is the set of all attributes shared by the objects O, and in the same time O is the set of all objects that have all attributes in A.

[2] Difunctional decomposition enables obtaining the isolated points of a binary relation through calculating the Fringe Relation. This fringe relation is, by definition, a difunctional relation, and all its elements are isolated points. Thus, the formal concepts can be easily obtained by finding such isolated points, since if (a, b) is an isolated point, by definition it is included in one concept only [33].

[3] Here compressible means that the generated spectrum $\boldsymbol{f}$ has a large number of frequencies whose entries (i.e., Fourier coefficients) have magnitudes that are small compared to the norm of $\boldsymbol{f}$ (i.e., the energy of $\boldsymbol{f}$).

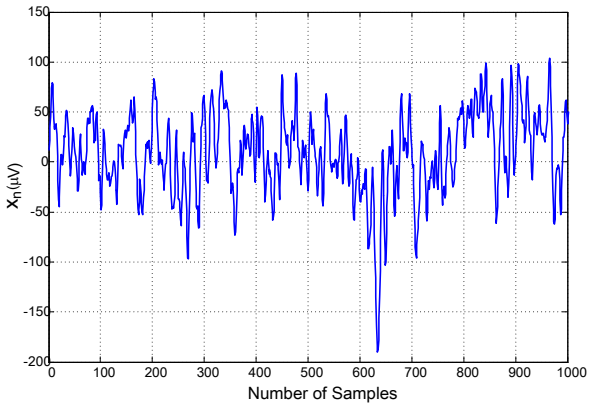

Fig. 4. An example of class Healthy EEG signal in the time domain.

consumption for such Fourier sparse signals through transmitting only energetic Fourier coefficients, while retrieving original signal at the receiver side.

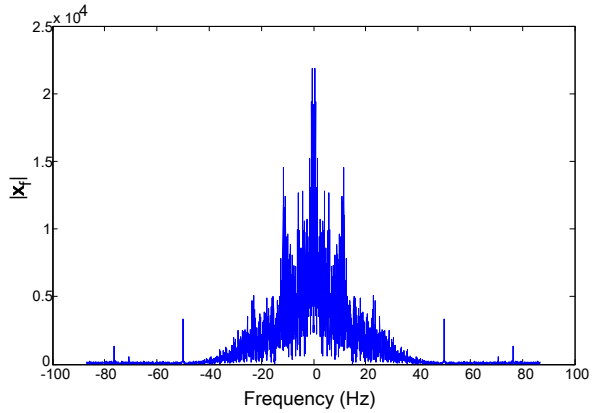

Fig. 5. An example of class Healthy EEG signal in the frequency domain.

B. Threshold-based Compression

Motivated by the EEG signal characteristics in the frequency domain, we update the OFDM transceiver architecture at the physical layer to support our compression scheme. Unlike the state-of-the-art compression techniques that are applied at the higher layers [10][17], we convey our compression scheme into the physical layer exploiting the existing OFDM transceiver's components in order to perform efficient compression without adding much complexity.

As mentioned, given the basic OFDM transceiver architecture in Figure 2, we have added two blocks in order to implement our TBC scheme, namely, the TBC and the FFT Vector Reconstruction. In the TBC block, leveraging the fact that several Fourier coefficients $\boldsymbol{x}_f$ of the EEG signal $\boldsymbol{x}$ have negligible magnitude (see Figure 6), we consider as 0s all symbols with magnitude lower than a predefined threshold δ (see Figure 8). The threshold is set according to the channel characteristics and the maximum distortion that can be tolerated at the receiver side. Clearly, the higher the value of δ, the larger the compression ratio and the resulting distortion. Then, whenever we have a number of consecutive zeros greater than two, the transmitter does not send them, but it notifies the receiver about the length of this sequence and its position in the stream of transferred data. We remark here that efficient techniques like run-length encoding [36] can be leveraged to perform such task.

At the receiver side, the FFT vector reconstruction block is responsible for adding zeros in the received vector at the positions of the ignored symbols before forwarding it to the FFT block. The latter will then demodulate the received symbols and reconstruct the EEG signal.

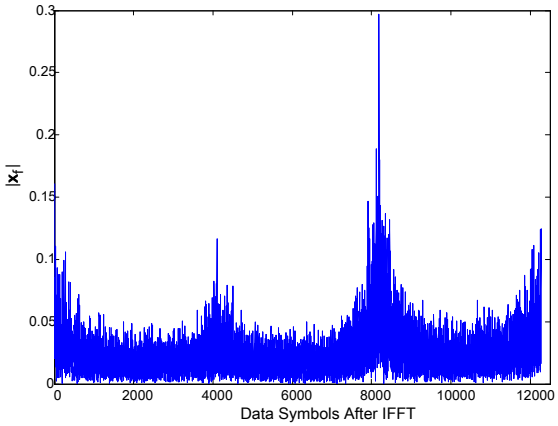

Fig. 6. Generated symbols after IFFT while considering 16-QAM modulation.

C. Error Correction

In order to quantify the achieved compression gain compared to the consequent signal distortion due to our compression scheme, we define the compression ratio as

$$C_r = \left(1 - \frac{\gamma}{\mu}\right) \times 100 \tag{9}$$

where γ is the number of data symbols to be transmitted, and μ is the number of the generated data symbols after modulation. While the signal distortion is quantified using Percent Root mean square Difference (PRD), which is given by

$$PRD = \sqrt{\frac{\sum_{i=1}^{N} [\boldsymbol{x}(i) - \boldsymbol{x}_r(i)]^2}{\sum_{i=1}^{N} [\boldsymbol{x}(i) - \bar{\boldsymbol{x}}]^2}} \times 100, \tag{10}$$

where $\bar{\boldsymbol{x}}$ is the average value of the original quantized signal, and $\boldsymbol{x}_r$ is the reconstructed one.

Interestingly, using our EEG compression transceiver we can easily define some of the wrong reconstructed samples at the receiver side. As shown in Figure 7, some of the wrong samples have very large amplitude compared to the correct samples. This advantage can be used as an Error Correction (EC) scheme in order to decrease Sample Error Rate (SER) and signal distortion at the receiver through: (i) identifying received samples with relatively large amplitude (samples with error), (ii) retransmitting the reconstructed samples with error.

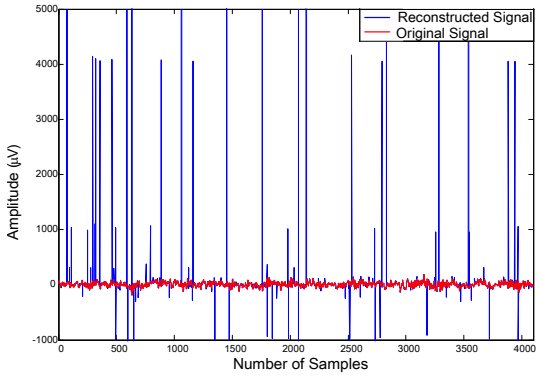

Fig. 7. A comparison between reconstructed and original EEG signal for healthy class.

Despite the achieved compression ratio using TBC, we found that it is of prominent importance to further analyze the effect of symbol mapping and modulation on EEG signal characteristics in order to enhance the compression ratio. As noted from Figure 5 and Figure 6, the EEG signal characteristics after modulation and IFFT modules have been changed and turned to be less compressible. This is mainly due to the effect of symbol mapping and modulation, since representing each data sample with multiple symbols turns the generated symbols after IFFT to be less compressible, i.e., most of the generated symbols after IFFT will have large magnitudes, thus, cannot be neglected. We will tackle this challenge in the next two sub-sections.

D. Higher-order Modulation

To tackle the problem of symbol mapping effect on EEG sparsity and increase compression efficiency of our transceiver, we study the characteristics of generated symbols after Fourier transform with and without symbol mapping and modulation (see Figure 6 and Figure 5). We find that exploiting higher-order modulation can help in increasing compression ratio of our transceiver through representing each EEG sample in one symbol, which relieves the effect of symbols mapping. However, as shown in Figure 8-(a), magnitudes of the generated symbols after IFFT $|\boldsymbol{x}_f|$ are still less compressible compared to the original case without modulation, i.e., in Figure 5 (even after considering the higher-order modulation). As a result, when applying our threshold-based compression, some of the important symbols may be also neglected. To avoid this, we apply *Symbols Masking* before compression. This masking is based on our prior knowledge about the EEG characteristics in the frequency domain. We define a window size W which is the percentage of compressible symbols relative to the total number of symbols. Using this masking, we define the less important symbols of $\boldsymbol{x}_f$ to be passed by the TBC scheme, while isolating more important symbols from compression (see Figure 8-(b)). Using such masking with higher-order modulation can significantly mitigate the effect of symbols mapping and modulation on EEG characteristics. By doing so, we could obtain higher compression ratio compared to initial TBC scheme with lower order modulation, as will be shown in simulation results.

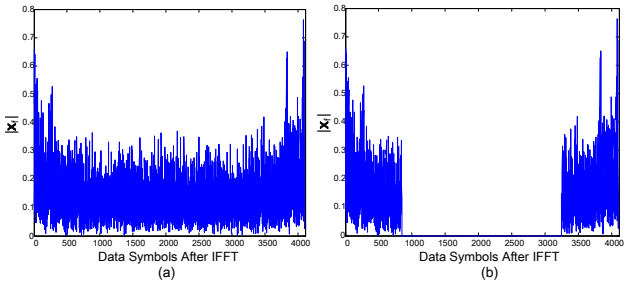

Fig. 8. Generated symbols after IFFT while considering 256-QAM modulation, (a) before compression, (b) after compression.

E. Steam-based Compression

Due to the quality of wireless channel, hardware design, or standards limitations, leveraging higher-order modulation may not be recommended in all cases. Thus, in order to make our transceiver adaptive for different channel conditions and modulation schemes, we propose a Stream-Based Compression (SBC) scheme. Leveraging the generated symbol streams in Section IV, the compression ratio can be further increased as follows. The independent streams of symbols are forwarded to the modulation and IFFT blocks, thus at TBC block, we can deal with each stream separately using different values of the δ threshold. This, as also shown in the simulation results section, yields a greater overall compression ratio.

For instance, using QPSK modulation and $L = 12$ bits, we will generate 6 streams of symbols. The symbols in each stream will have different values before modulation (see Figure 9) and after IFFT (see Figure 10). Thus, we can set per-stream thresholds so that each stream will be compressed as much as possible while still meeting the requirement on the maximum allowed distortion.

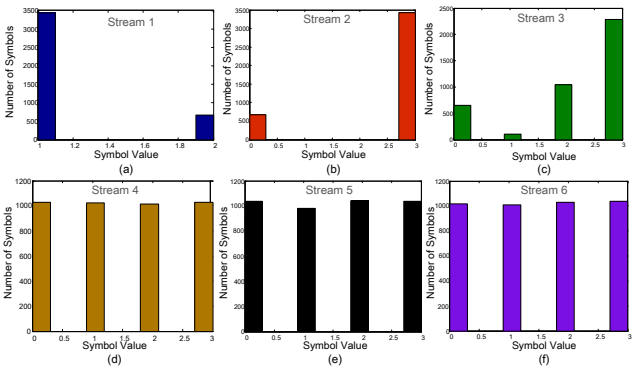

Fig. 9. Generated symbols' streams before modulation.

We remark that discovering the dependency between different streams and selecting only the independent streams is performed before IFFT (i.e., it pertains to the higher-layers of the transceiver architecture, while only the threshold-based compression is done after IFFT, i.e., in

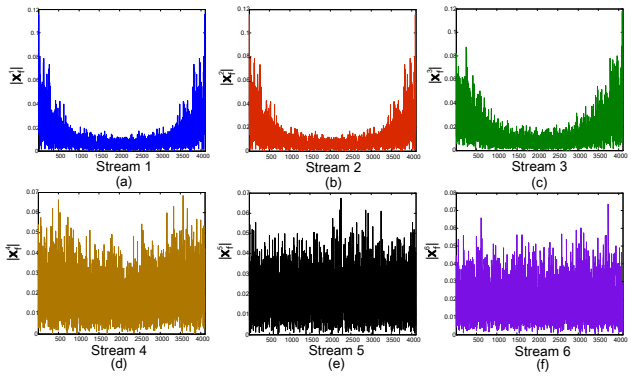

Fig. 10. Generated symbols' streams after IFFT while considering QPSK modulation.

the physical layers of the transceiver. Thus, to summarize, the main steps of our SBC scheme are as follows (see Figure 11):

- Higher-layers steps, which include stream creation, knowledge discovery, and defining the threshold δ, for individual streams.
- Physical-layer step, which includes TBC.

While at the receiver side, the inverse process is adopted through: (i) using FFT vector reconstruction, which is responsible for adding zeros in the received vector at the positions of the compressed symbols before forwarding it to the FFT, (ii) leveraging obtained dependency between different streams to retrieve discarded streams from transmission.

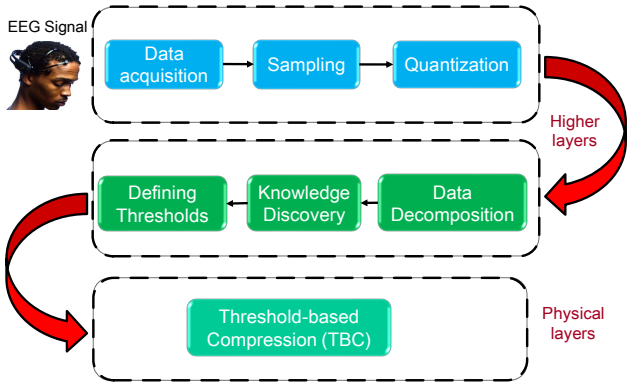

Fig. 11. The main steps of the proposed SBC scheme.

VI. Simulation Results and Discussion

In order to derive our simulation results, we implement the system model shown in Figure 1 and use the EEG dataset in [30]. Also, to quantify the performance gain provided by our solution, we investigate both the compression ratio and the consequent signal distortion, while considering high signal-to-noise ratio (SNR) for the wireless channel. The simulation parameters we used are reported in Table III.

First, we assess the performance of the proposed TBC transceiver in Section V without performing the signal decomposition into different symbol streams. Figure 12

TABLE III
Simulation Parameters

Parameter	T	N_s	T_s	L	M
Value	23.6 sec	4096	0.0058	12 bits	$\in \{2, 3, 4, 6\}$

shows the performance gain of the transceiver when the 16-QAM modulation (i.e., $M = 3$ symbols per sample) is used. Herein, we gradually increase the compression ratio C_r by increasing the threshold δ; furthermore, both the cases with and without our Error Correction (EC) scheme are considered. As expected, with increasing δ, the Sample Error Rate (SER) and signal distortion (PRD) increase as well (see Figure 12). However, when EC is applied, SER and PRD reduce significantly thanks to the retransmission of the erroneous samples. On the contrary, the actual or effective C_r decreases due to the higher retransmission overhead. Importantly, these results show that, using the well-known OFDM transceiver architecture with slight modifications, we can obtain about 25% compression ratio while keeping SER and distortion below 10%, which is acceptable by many applications.

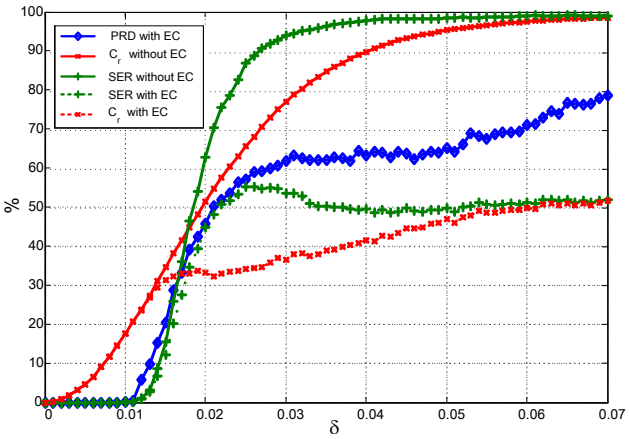

Fig. 12. Effect of varying C_r on signal distortion and SER when the TBC scheme and 16-QAM modulation are used.

Figure 13 highlights the increase in C_r that we can obtain by leveraging higher-order modulation and symbols masking. We can now achieve about 60% C_r while keeping distortion around 10%. Also, with larger window size W, the compression ratio grows at the expense of an increased signal distortion. We remark that, depending on the quality of the wireless channel, the modulation order can be increased (i.e., enabling high-order modulations for low channel errors), hence the compression ratio, while still meeting the application requirements.

Next, we assess the performance of the proposed SBC scheme in Section IV, i.e., we also account for the benefits brought by the decomposition of the signal into streams of symbols and their processing. Interestingly, our SBC transceiver can support both lossless and lossy compression. As depicted in Figure 14, we can achieve about 45% compression ratio at 0% SER and distortion, or about 55% compression ratio at less than 10% SER

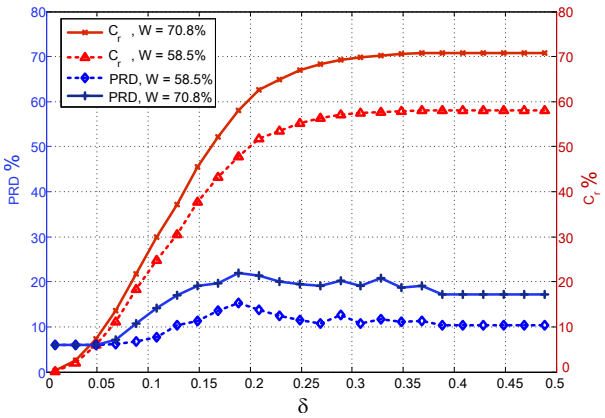

Fig. 13. Effect of varying the threshold δ on C_r and signal distortion using TBC scheme and 256-QAM modulation, for different window size W.

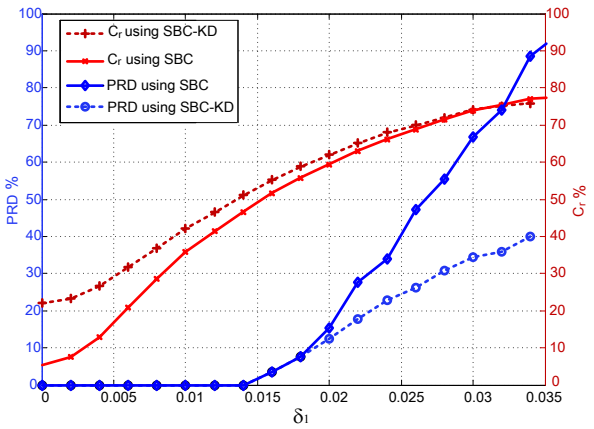

Fig. 15. Effect of knowledge discovery on enhancing compression ratio and signal distortion for QPSK modulation.

and distortion. Herein, we used the QPSK modulation with two compression thresholds δ_1 and δ_2, where δ_2 is fixed to 0.011 while δ_1 varies. In particular, δ_2 was used for stream 3, since its values have high variability before modulation and low amplitude after IFFT (see Figure 9 and Figure 10), while δ_1 was adopted for the other streams. Interestingly, such results show that, thanks to the signal decomposition into streams, we can significantly increase the compression ratio while applying low-order modulation schemes.

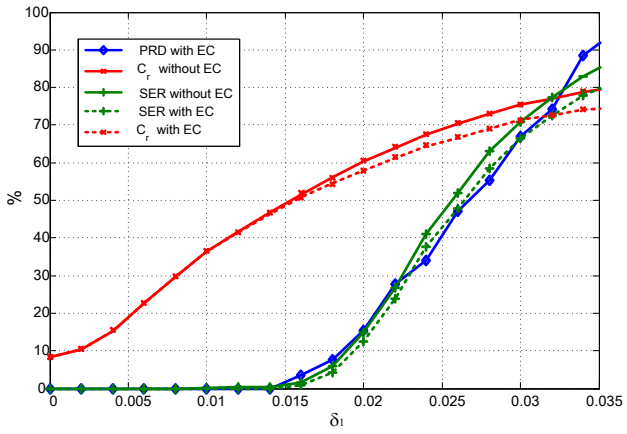

Fig. 14. Effect of varying threshold δ_1 on the compression ratio, signal distortion, and sample error rate, when the QPSK modulation is used.

The transceiver performance further improves if the SBC-KD scheme is used. Indeed, by applying knowledge discovery and transmitting only the minimal-representation streams, we can considerably resude the amount of transferred data while still accurately reconstructing the signal at the receiver side. The results in Figure 15 demonstrate that in this case we can obtain, roughly, 50% compression ratio at 0% SER and distortion, or 67% compression ratio with less than 20% distortion.

Finally, in Figure 16 we compare the performance of the proposed SBC-KD scheme with the DWT technique. Wavelet-based compression techniques consist of transmitting the most significant wavelet coefficients. The strategy adopted to select such coefficients is the main distinguishing factor of the algorithms proposed in the literature [17]. Comparing to DWT-Level thresholding [37], we obtain 13% reduction in the PRD for compression ratios up to 50%, while achieving 5% reduction in the PRD for higher values, namely, up to 80%, of the compression ratio. Furthermore, we can use the proposed scheme for lossless compression for compression ratios up to 50%, which shows significant gains over DWT in applications requiring zero distortion and high quality analysis of the vital signs.

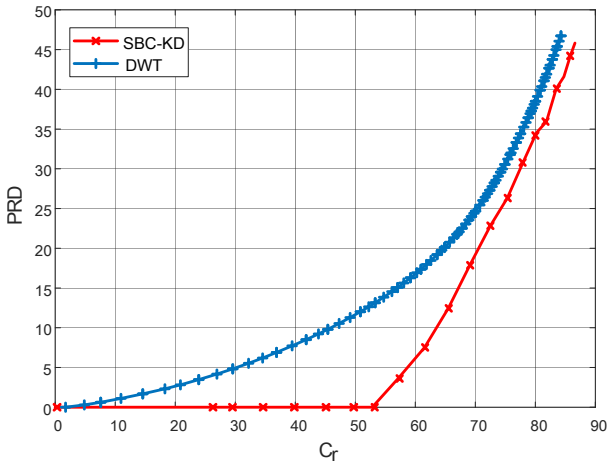

Fig. 16. Distortion variation for different values of compression ratio, for the proposed SBC-KD technique and the DWT-level thresholding scheme.

This achieved increase in compression ratio also reflects on the transmission energy consumption (see Table IV[4]). Thus, a significant amount of energy consumption can be saved using the proposed compression scheme. Also, as energy consumption decreases with increasing compression ratio and distortion, our scheme can be adapted to maintain the best tradeoff between energy consumption

[4]In Table IV, we leverage the energy consumption model presented in [38].

and signal distortion, based on application requirements and energy availability.

TABLE IV
TRANSMISSION ENERGY CONSUMPTION VS. COMPRESSION RATIO

Transmission Energy (mJ)	C_r %
163.84	0
147.46	10
114.69	30
65.54	60
49.15	70
24.58	85

VII. CONCLUSION

We proposed a novel transceiver design based on symbol-streams compression: the generated symbols are grouped into streams, and only streams that are independent of each other are compressed and transmitted. Additionally, streams are compressed separately, thus the compression thresholds can be tailored to each stream so that the compression ratio is increased while yielding low distortion. In this context, we focused on the case of the EEG signal and showed how the Fourier coefficients representing such signal can be effectively compressed while accounting for the wireless channel characteristics and the application requirements in terms of signal distortion. Notably, the proposed transceiver is compatible with the current 4G standard and the evolving requirements of next-generation networks since it relies on the OFDM technology with two simple added modules.

Our simulation results highlight the benefits of our solution in terms of overall compression ratio and signal distortion, with the remarkable result of 50% compression ratio at zero distortion and sample error rate.

ACKNOWLEDGMENT

This work was made possible by GSRA grant # GSRA2-1-0609-14026 and NPRP grant # 7 - 684 - 1 - 127 from the Qatar National Research Fund (a member of Qatar Foundation). The findings achieved herein are solely the responsibility of the authors.

REFERENCES

[1] Y. E. Gelogo and H. K. Kim, "Integration of wearable monitoring device and android smartphone apps for u-healthcare monitoring system," *International Journal of Software Engineering and Its Applications, vol. 9, no. 4*, pp. 195–202, 2015.

[2] O. Banos, C. Villalonga, M. Damas, P. Gloesekoetter, H. Pomares, and I. Rojas, "Physiodroid: Combining wearable health sensors and mobile devices for a ubiquitous, continuous, and personal monitoring," *The Scientific World Journal*, 2014.

[3] C. Thuemmler and C. Bai, "Health 4.0: application of industry 4.0 design principles in future Asthma management," *Springer International Publishing*, pp. 23–37, 2017.

[4] H. Adeli, S. Ghosh-Dastidar, and N. Dadmehr, "A wavelet-chaos methodology for analysis of EEGs and EEG subbands to detect seizure and epilepsy," *IEEE Transactions on Biomedical Engineering, vol. 54, NO. 2*, Feb. 2007.

[5] Y. Chae, J. Jeong, and S. Jo, "Toward brain-actuated humanoid robots: Asynchronous direct control using an eeg-based bci," *IEEE Transactions on Robotics*, vol. 28, no. 5, pp. 1131–1144, Oct 2012.

[6] F. Duan, D. Lin, W. Li, and Z. Zhang, "Design of a multimodal eeg-based hybrid bci system with visual servo module," *IEEE Transactions on Autonomous Mental Development*, vol. 7, no. 4, pp. 332–341, Dec 2015.

[7] A. J. C. Trappey, C. V. Trappey, U. H. Govindarajan, J. J. Sun, and A. C. Chuang, "A review of technology standards and patent portfolios for enabling cyber-physical systems in advanced manufacturing," *IEEE Access*, vol. 4, pp. 7356–7382, 2016.

[8] T. Moy, L. Huang, W. Rieutort-Louis, C. Wu, P. Cuff, S. Wagner, J. C. Sturm, and N. Verma, "An eeg acquisition and biomarker-extraction system using low-noise-amplifier and compressive-sensing circuits based on flexible, thin-film electronics," *IEEE Journal of Solid-State Circuits*, vol. 52, no. 1, pp. 309–321, Jan 2017.

[9] D. Craven, B. McGinley, L. Kilmartin, M. Glavin, and E. Jones, "Compressed sensing for bioelectric signals: A review," *IEEE Journal of Biomedical and Health Informatics*, vol. 19, no. 2, pp. 529–540, March 2015.

[10] J. Chiang and R. K. Ward, "Energy-efficient data reduction techniques for wireless seizure detection systems," *Sensors, 14(2)*, pp. 2036–2051, 2014.

[11] D. Rav, C. Wong, F. Deligianni, M. Berthelot, J. Andreu-Perez, B. Lo, and G. Z. Yang, "Deep learning for health informatics," *IEEE Journal of Biomedical and Health Informatics*, vol. 21, no. 1, pp. 4–21, Jan 2017.

[12] T. Strohmer, "Measure what should be measured: Progress and challenges in compressive sensing," *IEEE Signal Processing Letters*, vol. 19, no. 12, pp. 887–893, 2012.

[13] S. Acciarito, G. Cardarilli, L. D. Nunzio, R. Fazzolari, G. Khanal, and M. Re, "Compressive sensing reconstruction for complex system: A hardware/software approach," *Applications in Electronics Pervading Industry, Environment and Society, Springer, Cham*, vol. 429, pp. 192–200, 2016.

[14] B. L. Sturm and M. G. Christensen, "Comparison of orthogonal matching pursuit implementations," *Proceedings of the 20th European Signal Processing Conference (EUSIPCO)*, pp. 220–224, Aug 2012.

[15] C. Hegde, A. C. Sankaranarayanan, W. Yin, and R. G. Baraniuk, "Numax: A convex approach for learning near-isometric linear embeddings," *IEEE Transactions on Signal Processing*, vol. 63, no. 22, pp. 6109–6121, Nov 2015.

[16] Y. Wang, X. Li, K. Xu, F. Ren, and H. Yu, "Data-driven sampling matrix boolean optimization for energy-efficient biomedical signal acquisition by compressive sensing," *IEEE Transactions on Biomedical Circuits and Systems*, vol. 11, no. 2, pp. 255–266, April 2017.

[17] M. Hooshmand, D. Zordan, D. D. Testa, E. Grisan, and M. Rossi, "Boosting the battery life of wearables for health monitoring through the compression of biosignals," *IEEE Internet of Things Journal*, vol. 4, no. 5, pp. 1647–1662, Oct 2017.

[18] D. D. Testa and M. Rossi, "Lightweight lossy compression of biometric patterns via denoising autoencoders," *IEEE Signal Processing Letters*, vol. 22, no. 12, pp. 2304–2308, Dec 2015.

[19] N. Sriraam and C. Eswaran, "Performance evaluation of neural network and linear predictors for near-lossless compression of EEG signals," *IEEE Transactions on Information Technology in Biomedicine*, vol. 12, no. 1, pp. 87–93, Jan 2008.

[20] S. Lee, J. Kim, and M. Lee, "A real-time ecg data compression and transmission algorithm for an e-health device," *IEEE Transactions on Biomedical Engineering*, vol. 58, no. 9, pp. 2448–2455, Sept 2011.

[21] H. Daou and F. Labeau, "Dynamic dictionary for combined EEG compression and seizure detection," *IEEE Journal of Biomedical and Health Informatics*, vol. 18, no. 1, pp. 247–256, Jan 2014.

[22] G. Xu, J. Han, Y. Zou, and X. Zeng, "A 1.5-D multi-channel EEG compression algorithm based on NLSPIHT," *IEEE Signal Processing Letters*, vol. 22, no. 8, pp. 1118–1122, Aug 2015.

[23] E. S. G. Carotti, J. C. D. Martin, R. Merletti, and D. Farina*, "Compression of multidimensional biomedical signals with spatial and temporal codebook-excited linear prediction," *IEEE Transactions on Biomedical Engineering*, vol. 56, no. 11, pp. 2604–2610, Nov 2009.

[24] M. Kim and S. Chang, "A consumer transceiver for long-range IoT communications in emergency environments," *IEEE Transactions on Consumer Electronics*, vol. 62, no. 3, pp. 226–234, August 2016.

[25] S. Brandsttter and M. Huemer, "A novel MPSoC interface and control architecture for multistandard rf transceivers," *IEEE Access*, vol. 2, pp. 771–787, 2014.

[26] E. Schweiter and T. Minteer, "Fiber-optic transceiver for combined serial data and time code communication," May 18 1999, US Patent 5,905,758. [Online]. Available: https://www.google.tl/patents/US5905758
[27] G. Knox, "Wireless music and data transceiver system," June 29 2004, US Patent 6,757,913. [Online]. Available: https://www.google.com/patents/US6757913
[28] P. Guan, D. Wu, T. Tian, J. Zhou, X. Zhang, L. Gu, A. Benjebbour, M. Iwabuchi, and Y. Kishiyama, "5g field trials: Ofdm-based waveforms and mixed numerologies," *IEEE Journal on Selected Areas in Communications*, vol. 35, no. 6, pp. 1234–1243, June 2017.
[29] D. C. Alves, G. S. da Silva, E. R. de Lima, C. G. Chaves, D. Urdaneta, T. Perez, and M. Garcia, "Architecture design and implementation of key components of an OFDM transceiver for IEEE 802.15.4g," *IEEE International Symposium on Circuits and Systems (ISCAS)*, pp. 550–553, May 2016.
[30] R. Andrzejak, K. Lehnertz, C. Rieke, F. Mormann, P. David, and C. Elger, "Indications of nonlinear deterministic and finite dimensional structures in time series of brain electrical activity: Dependence on recording region and brain state," *Physical Review E, 64, 061907*, 2001.
[31] T.-D. Chiueh and P.-Y. Tsai, *OFDM Baseband Receiver Design for Wireless Communications*, 1st ed. John Wiley & Sons, 2007.
[32] M. Sarfraz, *Computer-Aided Intelligent Recognition Techniques and Applications*, 2nd ed. John Wiley & Sons, 2005.
[33] R. Khcherif, M. M. Gammoudi, and A. Jaoua, "Using difunctional relations in information organization," *Information Sciences 125*, pp. 153–166, 2000.
[34] Y. Li, Y. Yuan, X. Guo, Y. Sheng, and L. Chen, "A fast algorithm for generating concepts," *International Conference on Information and Automation*, pp. 1728–1733, June 2008.
[35] J. G. Proakis and D. G. Manolakis, *Digital signal processing: principles, algorithms and applications*, 4th ed. Pearson Prentice Hall, 2007.
[36] J. Trein, A. T. Schwarzbacher, B. Hoppe, and K. H. Noff, "A hardware implementation of a run length encoding compression algorithm with parallel inputs," *IET Irish Signals and Systems Conference (ISSC 2008)*, pp. 337–342, June 2008.
[37] A. Awad, M. Hamdy, A. Mohamed, and H. Alnuweiri, "Real-time implementation and evaluation of an adaptive energy-aware data compression for wireless EEG monitoring systems," *International Conference on Heterogeneous Networking for Quality, Reliability, Security and Robustness*, pp. 108–114, Aug 2014.
[38] J. Huang, F. Qian, A. Gerber, Z. M. Mao, S. Sen, and O. Spatscheck, "A close examination of performance and power characteristics of 4G lte networks," *Proceedings of the 10th international conference on Mobile systems, applications, and services*, pp. 225–238, June 2012.
[39] T. M.Cover and J. A.Thomas, *Elements of Information Theory*, 2nd ed. John Wiley & Sons, 2006.

APPENDIX

A. *Proof of Proposition* 1

We first obtain the best possible lossless compression based on the measurement of the information contained in our data streams through leveraging Shannon's entropy [39]. Let us represent the possible values of each stream by a discrete random variable x^m, where x^m is a discrete random variable taking values in $\{0, 1, \cdots, n\}$ with the i^{th} value occurs with probability p_i. The entropy $H(\boldsymbol{x}^m)$ of a stream $\boldsymbol{x}^m$ is defined as

$$H(\boldsymbol{x}^m) = -\sum_{i=1}^{n} p_i \log_2 p_i. \tag{11}$$

While the maximum entropy $H_{max} = \log_2(n)$. The reduction in the average uncertainty (information) of $\boldsymbol{x}^m$ relative to the maximum entropy H_{max} represents the boundaries of the performance of the strongest lossless compression possible for each stream. Hence, we define the maximum possible compression ratio of a stream $\boldsymbol{x}^m$ for lossless compression as:

$$\kappa^m = 1 - \frac{H(\boldsymbol{x}^m)}{H_{max}}. \tag{12}$$

Thus, the overall compression ratio for all streams is defined as

$$\kappa^s = \frac{\sum_{m=1}^{M}(\kappa^m)}{M}. \tag{13}$$

Since we decompose $\boldsymbol{x}$ into a linear sum of M streams, we will have

$$\boldsymbol{x} = \sum_{m=1}^{M} a_m \boldsymbol{x}^m, \tag{14}$$

where $a_m = 2^{mK}$. With such a decomposition, the entropy $H(\boldsymbol{x})$ of the original data without decomposition is defined as

$$H(\boldsymbol{x}) = H(\sum_{m=1}^{M} a_m \boldsymbol{x}^m), \tag{15}$$

where

$$H(\boldsymbol{x}) \geq \max\left\{H(\boldsymbol{x}^m)\right\}, \forall m \in \{1, 2, \cdots, M\} \tag{16}$$

with equality holds when $\boldsymbol{x}^m$'s have uniform distribution, leveraging the well-known entropy power inequality [39],

$$H(Z) \geq \max\left\{H(X), H(Y)\right\}, \tag{17}$$

for X, Y are two independent random variables, and their sum is $Z = X + Y$. From (16), and using appropriate manipulations, we can write the relationship of compression ratio as

$$1 - \frac{H(\boldsymbol{x})}{H_{max}} \leq \frac{\sum_{m=1}^{M}\left(1 - \frac{H(\boldsymbol{x}^m)}{H_{max}}\right)}{M}. \tag{18}$$

Now, from (12), (13), and (18), it can be easily noticed that $\kappa^t \leq \kappa^s$, where κ^s and κ^t are the maximum lossless compression ratio with and without decomposition, respectively.